

7) Divide by rod density to obtain the N° of photoisomerizations/individual rod

$$R^* \text{ photoR}^{-1} \text{ s}^{-1} = \frac{\text{Total } R^* \text{ photoR}}{\text{photoR density}}$$

(The assumption is that absorption by other than rhodopsin rods represents negligible fractions of the total absorption).

As it becomes evident from the equations above, the number of $R^* \text{ rod}^{-1} \text{ s}^{-1}$ depends on the dimensions and geometry of the experimental arena and stimuli used. Thus, the values need to be calculated independently for every experimental situation and are not readily convertible into photometric units, even in cases in which the ambient illumination measured, for example, in cd/m^2 would be the same for different experiments. The values used for *Rana temporaria* in the phototaxis experiments are as follows:

$$A_{\text{pupil}} = 10 \text{ mm}^2 \text{ [13]}$$

$$r = 0.45 \text{ cm [15]}$$

$$R = 26 \text{ cm}$$

$$\tau_{\text{media}} \approx 1 \text{ [14]}$$

$$OD_{\text{retina}} = 0.34 \text{ [16]}$$

$$D_{\text{stim}} = 7 \text{ cm}$$

$$\tau_{\text{cornea}} = 0.91 \text{ [15]}$$

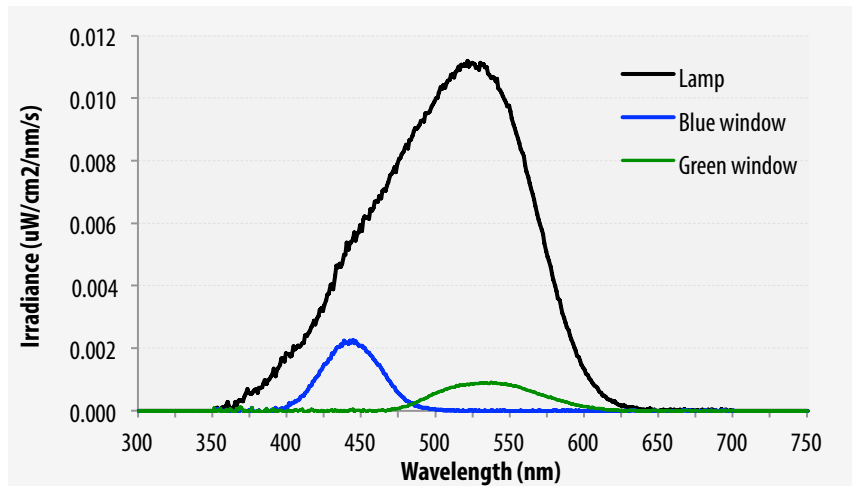
$$\gamma = 0.66 \text{ [17]}$$

$$A_{\text{retina}} = 1.13 \text{ mm}^2$$

7. STIMULI FOR PHOTOTAXIS EXPERIMENTS

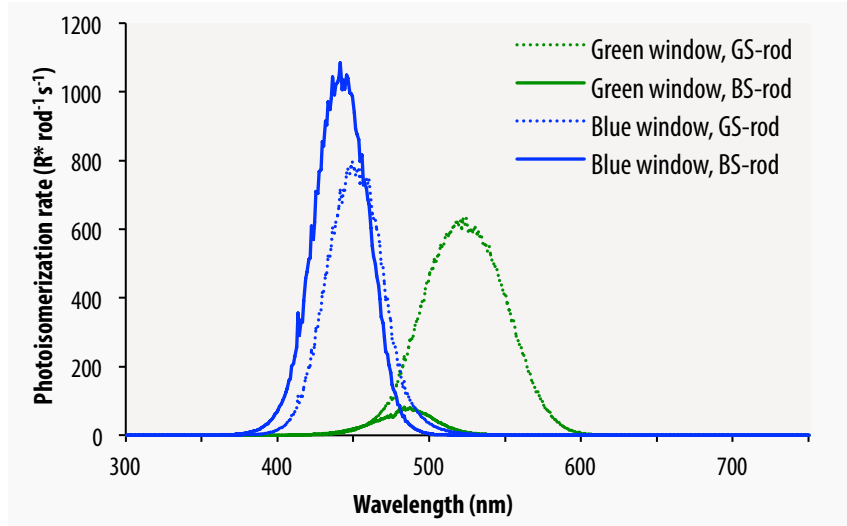
The irradiance spectra of the light source and the light passing through the filters used in these experiments are shown in Supplementary Figure 7.1.

The photoisomerization rates produced by the two windows (blue and green) in the two types of rods (BS and GS) are shown as stimulus spectra [$R^* \text{ rod}^{-1} \text{ s}^{-1} \text{ nm}^{-1}$] in Supplementary Figure 7.2. The total photoisomerization rate [$R^* \text{ rod}^{-1} \text{ s}^{-1}$] in each case is obtained as the integral of the respective spectrum (the area under the curve). The light intensities of the two windows were independently adjusted with neutral density filters so that both produced approximately equal rates of photoisomerizations in GS-rods, as given in Supplementary Table 8.1. The rates in BS-rods are then inevitably fixed by the spectral characteristics of the colour filters (Wratten N°8, “green” and N° 98, “blue”; Eastman Kodak Company USA). The filters were basically selected with the aim that BS-rod stimulation by the green filter should be negligible, whereas GS- and BS-rod stimulation by the blue filter should be equal. This could not be perfectly achieved given the limited complement of Wratten filters available: rather than the ideal BS/GS-rod stimulation ratios of 0 (green) and 1 (blue), the actual ratios were about 0.05 (green) and 1.3 (blue). We think these deviations from the ideal are in practice negligible at the low light levels that are of main interest in this study of rod-based colour discrimination ($\leq 1 R^* \text{ rod}^{-1} \text{ s}^{-1}$). It is worth noting that the smallest *achromatic* difference that a frog can detect at the lowest light levels (the increment threshold) is 100%, i.e., doubling the intensity of a very dim background light [13].



Supplementary Figure 7.1. Irradiance of the light source and filters used in phototaxis experiments.

Supplementary Figure 7.2. Photoisomerization rates ($R^* \text{ rod}^{-1} \text{ s}^{-1} \text{ nm}^{-1}$) produced in GS- and BS-rods by the “green” and “blue” stimuli used in the phototaxis experiments, measured at the maximum light intensity. Adjustment of the general illumination with neutral density filters means that all spectra are scaled down by a common factor in each experimental condition. The area under each curve yields total $R^* \text{ rod}^{-1} \text{ s}^{-1}$.



8. COMPLETE DATASETS FROM PHOTOTAXIS EXPERIMENTS

The output from the infrared jump-recording system was processed to yield the total jump counts shown in Supplementary Table 8.1. These data were used for statistical analysis of jump distributions by χ^2 testing: (1) jumps towards lit sectors (green + blue) vs. dark sectors; (2) jumps towards blue vs. green. In both cases the “expected” (random) distributions are 1:1.

Intensity ($R^* \text{ rod}^{-1} \text{ s}^{-1}$)	Animals	Blue jumps	Green jumps	Dark jumps	χ^2 test (Light vs. Dark)	χ^2 test (Blue vs. Green)
Darkness	15	163	193	355	$p > 0.05$	$p > 0.05$
0.001	15	247	404	536	$p < 0.001$	$p < 0.001$
0.03	17	359	732	911	$p < 0.001$	$p < 0.001$
0.3	17	528	995	958	$p < 0.001$	$p < 0.001$
3.01	17	1085	1453	915	$p < 0.001$	$p < 0.001$
30.12	17	1536	1485	898	$p < 0.001$	$p > 0.05$
301.18	17	1567	1250	698	$p < 0.001$	$p < 0.001$
30118.04	17	1896	1327	634	$p < 0.001$	$p < 0.001$

Supplementary Table 8.1. Raw data and statistics from phototaxis experiments at different light intensities. The p values marked in red indicate the cases in which the number of jumps towards each of the compared conditions was statistically significantly different.

To ease visualization of the data, the absolute jump counts of each frog were used to calculate the fractions of jumps made by that individual towards each of the sectors at each light intensity (number of jumps towards that sector divided by the total number of jumps of that individual at that intensity). Means \pm SEMs of the fractions were calculated across all frogs for each light intensity; these values are shown in Supplementary Table 8.2 and displayed as data points and error bars in Fig. 3B.

Intensity ($R^* \text{ rod}^{-1} \text{ s}^{-1}$)	Fraction Blue	Blue SEM	Fraction Green	Green SEM	Fraction Dark	Dark SEM	Fraction Light	Light SEM
Darkness	0.19813	0.0487	0.20866	0.06672	0.59322	0.07273	0.40678	0.07273
0.001	0.24774	0.03737	0.31622	0.02549	0.43604	0.04167	0.56396	0.04167
0.03	0.18229	0.0267	0.37968	0.03329	0.43803	0.03577	0.56197	0.03577
0.3	0.23771	0.02117	0.46574	0.02814	0.29655	0.02303	0.70345	0.02302
3.01	0.32445	0.02257	0.46793	0.02404	0.20762	0.0232	0.79238	0.0232
30.12	0.45132	0.02935	0.34107	0.02541	0.20761	0.03073	0.79239	0.03073
301.18	0.51833	0.02754	0.31623	0.02542	0.16544	0.01906	0.83456	0.01906
30118.04	0.49902	0.02411	0.36363	0.01933	0.13735	0.01367	0.86265	0.01367

Supplementary Table 8.2. Results of phototaxis experiments at different light intensities expressed as mean values across frogs of the fractions of jumps calculated separately for each frog, and standard errors of the means. This dataset was used to build Figure 3B in the article.

9. REFERENCES

- [1] Govardovskii VI, Fyhrquist N, Reuter T, Kuzmin DG & Donner K. 2000 In search of the visual pigment template. *Visual neuroscience* **17**, 509-528.
- [2] Warrant EJ & Nilsson DE. 1998 Absorption of white light in photoreceptors. *Vision Res* **38**, 195-207. (doi:10.1016/S0042-6989(97)00151-X).
- [3] Harosi FI. 1975 Absorption spectra and linear dichroism of some amphibian photoreceptors. *The Journal of general physiology* **66**, 357-382.
- [4] Aho AC, Donner K, Helenius S, Larsen LO & Reuter T. 1993 Visual performance of the toad (*Bufo bufo*) at low light levels: retinal ganglion cell responses and prey-catching accuracy. *J Comp Physiol A* **172**, 671-682.
- [5] Nilsson SE. 1964 An Electron Microscopic Classification of the Retinal Receptors of the Leopard Frog (*Rana pipiens*). *Journal of ultrastructure research* **10**, 390-416.
- [6] Donner K, Firsov ML & Govardovskii VI. 1990 The frequency of isomerization-like 'dark' events in rhodopsin and porphyropsin rods of the bullfrog retina. *The Journal of physiology* **428**, 673-692.
- [7] Hemila S & Reuter T. 1981 Longitudinal spread of adaptation in the rods of the frog's retina. *The Journal of physiology* **310**, 501-528.
- [8] Koskelainen A, Hemila S & Donner K. 1994 Spectral sensitivities of short- and long-wavelength sensitive cone mechanisms in the frog retina. *Acta physiologica Scandinavica* **152**, 115-124. (doi:10.1111/j.1748-1716.1994.tb09790.x).
- [9] Maximov VV, Orlov OY & Reuter T. 1985 Chromatic Properties of the Retinal Afferents in the Thalamus and the Tectum of the Frog (*Rana-Temporaria*). *Vision Res* **25**, 1037-1049. (doi:10.1016/0042-6989(85)90092-6).
- [10] Rohlf FJ & Sokal RR. 1995 *Statistical tables*, Macmillan.
- [11] Johnsen Sn. 2012 *The optics of life : a biologist's guide to light in nature*. Princeton, NJ, Princeton University Press; x, 336 p., 338 p. of plates p.
- [12] Roth LS, Balkenius A & Kelber A. 2007 Colour perception in a dichromat. *The Journal of experimental biology* **210**, 2795-2800. (doi:10.1242/jeb.007377).
- [13] Aho AC, Donner K & Reuter T. 1993 Retinal origins of the temperature effect on absolute visual sensitivity in frogs. *The Journal of physiology* **463**, 501-521.
- [14] Govardovskii VI & Zueva LV. 1974 Spectral sensitivity of the frog eye in the ultraviolet and visible region. *Vision Res* **14**, 1317-1321.
- [15] Aho AC, Donner K, Hyden C, Reuter T & Orlov OY. 1987 Retinal Noise, the Performance of Retinal Ganglion-Cells, and Visual Sensitivity in the Dark-Adapted Frog. *J Opt Soc Am A* **4**, 2321-2329. (doi:10.1364/Josaa.4.002321).
- [16] Donner K, Koskelainen A, Djupsund K & Hemila S. 1995 Changes in retinal time scale under background light: observations on rods and ganglion cells in the frog retina. *Vision Res* **35**, 2255-2266.
- [17] Dartnall HJ. 1968 The photosensitivities of visual pigments in the presence of hydroxylamine. *Vision Res* **8**, 339-358.